CARBON 3482
2 March 2005 Disk Used
ARTICLE IN PRESS
No. of Pages 9, DTD = 5.0.1

Available online at www.sciencedirect.com
SCIENCE DIRECT®

Carbon xxx (2005) xxx–xxx

CARBON

www.elsevier.com/locate/carbon

Unusually tight aggregation in detonation nanodiamond: identification and disintegration

A. Krüger [a,b], F. Kataoka [c,d], M. Ozawa [b,e], T. Fujino [c], Y. Suzuki [c], A.E. Aleksenskii [f], A. Ya. Vul' [b,f], E. Ōsawa [b,c,*]

[a] *Institut für Organische Chemie, Universität Kiel, Otto-Hahn-Platz 3, 24098 Kiel, Germany*
[b] *Department of Knowledge Based Information Engineering, Toyohashi University of Technology, Toyohashi, Aichi 441-8580, Japan*
[c] *NanoCarbon Research Institute, 304 Toudai Venture Plaza, 5-4-19 Kashiwa-no-Ha, Kashiwa, Chiba 277-0882, Japan*
[d] *Products Development Centre, Futaba Corporation, 1080 Yabutsuka, Chosei-mura, Chosei-gun, Chiba 299-4395, Japan*
[e] *Department of Integrated Biosciences, The University of Tokyo, Bunkyo-ku, Tokyo 113-8656, Japan*
[f] *Ioffe Physico-Technical Institute, 26 Polytechnicheskaya, St. Petersburg 194021, Russia*

Revised 10 February 2005; accepted 10 February 2005

Abstract

A remarkable observation that detonation of oxygen-deficient explosives in an inert medium produces ultra-fine diamond particles having diameters of 4–5 nm was made four decades ago, but this novel form of diamond has never been isolated in pure form thereafter. The reason for the difficulty was that the core aggregates having a diameter range of 100–200 nm are extremely tight and could not be broken up by any known method of de-aggregation. After a number of futile attempts, we were able to obtain primary particles by using the recently emerging technique of stirred-media milling with micron-sized ceramic beads. The milled aqueous slurry of nanodiamond gave a stable, thick and dark-coloured colloidal solution. After light sonication, dynamic light scattering measurements gave a sharp distribution in the single-digit nano-range, and HRTEM indicated separate particles having diameters of 4–5 nm, which agreed with the X-ray value of 4.4 nm for the primary particles. A model is presented for the core aggregates, which resembles the well-known grape-shaped 'aggregate structure' of the hardest type of carbon black.

Keywords: Diamond; Modelling, Electron microscopy, X-ray diffraction; Particle size

1. Introduction

In 1963 a group of Soviet scientists discovered single crystals of cubic diamond particles in soot produced by detonating an oxygen-deficient TNT/hexogen composition in inert media without using any extra carbon source (Fig. 1) [1,2]. The average size of crystals has been determined to be 4–5 nm from the half-widths of X-ray diffraction peaks [2,3]. The discovery offered a remarkably advantageous method of producing novel 'dispersed ultrananocrystalline diamond' (DUNCD according to Gruen's nomenclature [4]).

Although the historic discovery was kept secret for unduly long time for security reasons [5], research activities in this novel diamond increased sharply within the ex-Soviet countries after the first report was published in 1988 [6] and even industrial production was soon started in Siberia [2, see also Section 2.1 below]. However, the primary particles remained un-identified, this class of man-made diamond never attracted much attention in the western countries [7–9] and the industrial production was shortly suspended. All these problems were caused by the continued failure in disintegrating nanodiamond

* Corresponding author. Tel.: +81 471 408 671; fax: +81 4 7140 8893.
E-mail address: osawaeiji@aol.com (E. Ōsawa).

0008-6223/$ - see front matter © 2005 Published by Elsevier Ltd.
doi:10.1016/j.carbon.2005.02.020

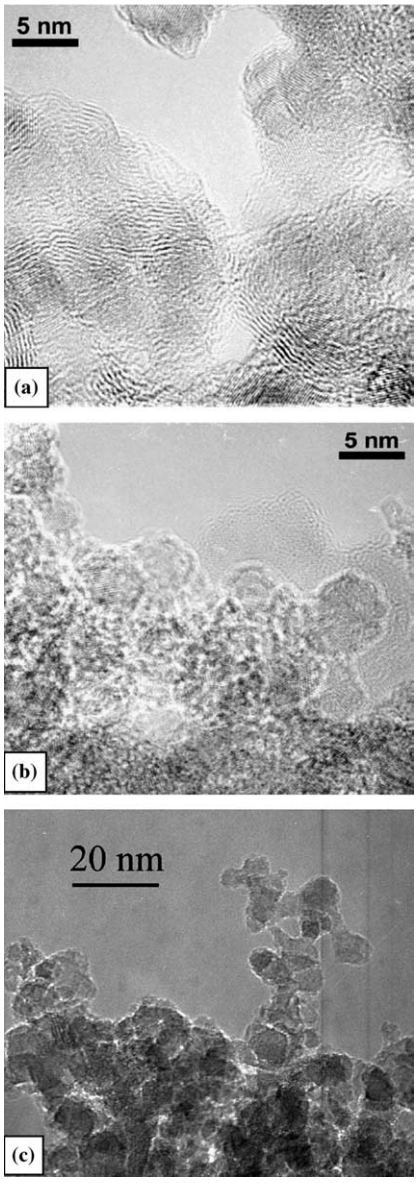

Fig. 1. TEM photographs (200 keV) of nanodiamond aggregate (NDA): (a) pristine *N2* (soot, see Table 1), (b) pristine *N4* (after washing with hot nitric acid), (c) a recent commercial product *B′*.

aggregates (NDA) into primary particles. Researchers have often remarked on the peculiar modes of aggregation in the NDA, and even briefly discussed about the presence of extremely tight core [10–14], which seemed to be of different nature from the conventional aggregates that occur due to the active surface of small particles [15–17]. Nevertheless, no systematic study on the persistent aggregation in the NDA has been reported in the past. Stimulated by the recent discovery of higher diamondoid molecules from petroleum gas [18], we began seeking ways of isolating the smallest nanodiamond crystals from the detonation soot.

In this paper we briefly describe the nature of differential aggregation modes in NDA as studied by the combination of dynamic light scattering (DLS), HRTEM and SEM, present a model for the core aggregate and disclose the only practicable method that we find to break up the latter to release the long-wanted primary particles.

2. Experimental

2.1. Materials

NDA samples *N1–N4* (Table 1) were prepared in our laboratory in St. Petersburg following an industrial procedure [19] by detonating Composition B, a 65:35 mixture of 2,4,6-trinitrotoluene (TNT) and hexahydro-1,3,5-trinitro-1,3,5-triazine (hexogen) in an atmosphere of carbon dioxide (dry synthesis) or in water (wet synthesis). In dry synthesis, fresh soot was collected from the wall of the detonation chamber and ploughed with magnets to remove magnetic constituents that had been cleaved off from the chamber wall by the shock of detonation. Other visible foreign materials were removed by passing an aqueous suspension of the magnet-processed soot through a columnar sieve with a mesh size of 0.25 mm, and the sieved suspension allowed to stand for 24 h. Settled soot was collected by decantation, and dried at 120 °C in air for 12 h to obtain raw soot (*N1*). In the case of wet synthesis, the aqueous suspension of raw soot was filtered through sieve and processed as mentioned above, ground in a mortar, sieved once again, and dried to give raw soot (*N2*). The raw soot

Table 1
Elementary analysis of diamond-containing raw soot and crude nanodiamond aggregates (NDA)

Sample	Note	n[a]	C	H	N	O	Ash[b]
Before oxidative purificatioin							
N1	Soot[c], CO_2[d]	5	89.67	0.78	2.77	3.14	3.64
N2	Soot[c], H_2O[d]	3	89.29	2.78	3.20	3.18	1.55
B″	Soot[c], 2003	2	89.40	1.50	3.35	3.72	2.03
After oxidative purification							
N3	CO_2[d]/HNO_3 50%, 200 °C[e]	4	86.83	0.91	2.45	9.73	0.08
N4	CO_2[d]/HNO_3 70%, 250 °C[e]	5	85.26	0.98	2.45	10.42	0.89
Commercial products							
A	1999[f]	3	83.94	0.94	2.18	10.50	2.39
B	2001[f]	3	85.63	1.77	2.12	9.01	1.47
B′	2003[f]	4	89.84	1.01	2.20	5.76	1.19

[a] Number of analysis.
[b] Non-volatile components.
[c] Crude reaction mixture subjected to magnet treatment and sieving, no oxidative purification.
[d] Detonation medium, either CO_2 or water.
[e] Oxidative purification by means of hot nitric acid.
[f] The year of import.

thus collected was heated in an autoclave for 30 min in air for 12 h.

Commercial NDA samples were purchased from two sources, Federal Science-Production Centre "ALTAI", Biisk, Siberia, Russia (designated below as *A*), and Gansu Lingyun Nano-Material Co., Ltd., Lanzhou, China (designated *B*, *B*′) in order to supplement the laboratory samples. *A* is dark brown whereas *B*, *B*′ appear light grey. Raw soot from the latter manufacturer was also examined (*B*″). Commercial NDAs were used mainly for milling experiments [20].

2.2. Apparatuses and analyses

Transmission electron micrographs were taken on JEOL JEM2010 and JEM2010F microscopes operating at 200 keV acceleration voltages and a Hitachi H7100 operating at 125 keV. SEM images were recorded using a JSM6300 scanning electron microscope at 20 kV acceleration voltages on a support of graphitic carbon tape. Infrared spectra were recorded on a JASCO FT/IR-610 Fourier Transform Infrared Spectrometer. In order to avoid inclusion of humidity the samples were prepared using the modified KBr pellet technique: the sample powder was ground in an agate mortar under inert atmosphere and quickly pressed between two thin plates of KBr (available from JASCO) in a special mini-press to obtain an air-tight specimen ready for mounting

Quantitative X-ray analyses were performed on a Rigaku Geigerflex D-Max/RC diffractometer using CuK_α radiation with $\lambda = 1.542$ Å. Diamond carbon was determined by evaluating diffraction intensity from (1 1 1) plane using sodium fluoride as internal standard [21]. Commercial micron-sized powder of natural diamond (Aldrich Catalogue No. 48359-1, C 99.42%) was used as the reference for calibration (correlation coefficient = 0.9999). A mixture of precisely weighed NDA sample and NaF was thoroughly ground in an agate mortar with silicon grease, pasted over a non-reflectance sample holder, and diffraction intensities of two non-overlapping diffraction peaks at $2\theta = 38.3$–39.4 (NaF) and 40.0–48.0 [diamond (1 1 1)] were integrated five times. The mixing/integration step was repeated 4–5 times. Diamond contents (standard deviation of errors) thus obtained for commercial NDAs *A*, *B* and *B*′ were 61.3% (5.1), 70.8% (4.7) and 76.8% (1.2), respectively.

Particle Analyzer FPAR1000 from Otsuka Electronics Co., based on DLS method [22,23] and equipped with a 658 nm semiconductor laser, was used to obtain optical particle-size distribution between 3 nm and 5 μm. Sonication was carried out in a supersonic washing bath (Elma GmbH, Transsonic Digital S, type T490DH, 240 W, 40 kHz), or with direct-immersion sonicators equipped with a conical titanium sonotrode with 3 mm in diameter at the tip (Ultrasonic Processors, Dr. Hielscher GmbH, UP400S, 400 W, 24 kHz and UIP1000, 1 kW, 20 kHz), or high-power sonicators equipped with titanium sonotrods, 46 $\phi \times 384$ mm (Ultrasonic System, Telesonic Co., SRR and GRR, 2 kW, 20 kHz).

Elemental analyses were carried out at the Centre for Organic Elemental Microanalysis, Faculty of Pharmaceutical Sciences, Kyoto University, Japan (Table 1).

2.3. Stirred-media milling

Disintegration of DNA to primary particles was performed by milling with micron-sized ceramic beads using a self-made vertical stirred mill consisting of a 25 ml Teflon vessel, and a multi-bladed Teflon agitator connected to a high-speed motor at the Netsuren Co., Hiratsuka. Prior to milling, NDA was subjected to preliminary comminution with a small atomizer, Robomix F manufactured by Tokushu-Kika Co. Plasma-processed spherical silica-beads with 0.1 mm in diameter (manufactured by Netsuren Co.) were charged to the extent of 70% of the vessel volume, and a 2 wt.% suspension of NDA in pure water added to fill the rest of the vessel volume. The mill was tightly closed with cover, and the content agitated at a peripheral speed of 10 m/s between 10 min up to 3 h under cooling with running water. At the end of milling, beads were separated by filtration and/or centrifugation and the slurry diluted with water to 0.2% concentration and subjected to sonication to obtain a clear colloidal solution of de-aggregated nanodiamond. Milling conditions are not optimized.

3. Results

3.1. Assessment of purity

Quantitative analysis of diamond contents of NDAs was performed only on commercial products because of the large sample-size required (ca 0.5 g). Diamond contents of *A*, *B* and *B*′ obtained in this way increased from 62% to 77% with the year of production (see Section 2). Elemental analyses of the samples used (Table 1) reveal significant amounts of hetero-atoms (H, N, O) and ashes in addition to carbon. Newer products give higher carbon, and lower oxygen and ash contents. These results attest to the advancing production technology during the past few years.

Infrared spectra(Table 2)provide some insight into the state of heteroatoms. Broad absorption of associated hydroxyl groups at ~3430 cm^{-1} (ν_{OH}) is the most intense in all the samples studied (2nd column). The corresponding bending mode (δ_{OH}) at ~1635 cm^{-1} showed up as well in all cases (5th column). We cannot estimate the oxygen attached to diamond due to the possible contamination with amorphous carbon, which may carry oxygen atoms, too. In spite of this uncertainty, the most likely source of oxygen in NDA seems to be nitric acid

Table 2
IR signals in the samples of detonation nanodiamond[a]

No.	ν_{OH} (assoc.)	ν_{CH} (Csp^3–H)	$\nu_{C=O}$ (saturated ketone)	δ_{OH} (assoc.)	δ_{CH} (Csp^3–H)	δ_{COH} (alcohol)	$\nu_{C\text{-}O}$(alcohol)
N1	3435vsbr	Trace	–	1637s		–	–
N2	3435vsbr	2919m 2851m	–	1633m	1460w	–	–
N3	3433vsbr	Trace	1729ms	1628s	–	1416w,1384s	–
N4	3427vsbr	Trace	1768m[d] 1707m	1632m	–	1361mw	–
A	3427vsbr	Trace	1759m	1628s	–	1384m	1128mbr
B	3432vsbr	2954sh 2923s 2854m	1781m[d]	1626m	1459w	–	1114mbr
Standard[b]	3600–3100	[c]	1745–1715	1630–1615	[e]	1410–1310	1200–1100

[a] vs = very strong, s = strong, m = medium, w = weak, vw = very weak, sh = shoulder, br = broad.
[b] Socrates G. Infrared characteristic group frequencies. Chichester: Wiley; 1980. p. 45–6 unless otherwise noted.
[c] Ref. b:28 (as,CH_3) 2975–2950, (s,CH_3) 2885–2865; (as, CH_2) 2940–2915, (s,CH_2) 2870–2840.
[d] Abnormally high for ketones. Probably assignable to γ-lactone (ref. b:73) or $\alpha \times \beta$ unsaturated ester (ref. b: 68–71).
[e] Ref. b:28 (as,CH_3) 1465–1440; (scissor,CH_2) 1480–1440.

used for the removal of soot at the end of the explosion experiment (see Section 2.1). The reaction intermediates containing alcohol and ketone groups on the surface of diamond particles are always left on the surface of particles when the oxidation reaction is terminated:

$$C \xrightarrow{HNO_3} C\text{–}O\text{–}NO_2 \underset{-HNO_3}{\overset{H_2O}{\rightarrow}} C\text{–}OH \xrightarrow{\text{oxidation}} C{=}O \qquad (1)$$

Emergence of carbonyl (4th column of Table 2, 1707–1781 cm^{-1}) and alcoholic C-OH bending (7th column, 1416–1361 cm^{-1}) absorptions in the acid-washed products (*N3*, *N4*, *A* and *B*) supports this interpretation. Strong hydroxyl IR absorptions also appear in the raw soot (*N1* and *N2*), and this fact indicates an alternative but ready route to incorporating hydroxyl groups, probably by nucleophilic attack of water molecule in the slurry or in the washing media to free spins generated during milling.

Sharp $C_{sp}3$-H stretching absorptions appear just below 3000 cm^{-1} together with a weak bending band at 1460 cm^{-1} in *N2*. As *N2* is the only sample prepared by wet synthesis among the laboratory-made samples studied (Table 1), we assume that C_{sp} 3-H bonds enter into *N2* by proton abstraction from water by surface carbon radicals. Infrared spectra do not show any sign of nitrogen-containing functional groups like nitrate ester (Eq. (1)), cyano or amide groups. It is likely that nitrogen is not located at the particle surface, but buried within the crystal lattice of diamond as in other natural and artificial diamonds [7]. The abnormally high content of nitrogen in detonation nanodiamonds (2.5%) compared to natural diamonds (ppm orders) most likely arises from the high content of nitro groups in the explosives used.

3.2. Identification of aggregates

According to DLS analysis, NDA samples commonly consist of three discrete size-groups of aggregates, centred around 100–200 nm, 2–3 μm and 20–30 μm, in the increasing abundance, but no NDA sample that we studied here exhibits any sign of distribution in the 3–10 nm region expected for primary particles. For example, pristine samples, *N4* and *A* (Fig. 2), are dominated by the largest size-group, or agglomerates, so are all other NDAs manufactured in the same way. The measured diameters of the largest agglomerates are out of the guaranteed range for the particle analyzer used, but SEM photographs do show particles corresponding to this size range (Fig. 3a). Treatment of the agglomerates in a weak supersonic generator of washing-bath type readily destroys them into the intermediate aggregates (Figs. 2 and 3b), which in turn seems to simultaneously equilibrate with the smallest, or core aggregates. With more powerful sonication the equilibration is completely shifted to the core aggregates in short time. For example, immersion of a 2 kW Ultrasonic Generator into a circulating bath of 0.1 wt.% *A* produced slightly cloudy but mono-disperse suspensions with an average size of 120 nm in a few minutes.

It is likely that the agglomerates and intermediate aggregates are both formed during the final drying stage of production. However, the core aggregates are clearly shown to be extremely tight, and seems to have been generated before the drying process. After a number of failed attempts using various kinds of supersonic generators (see Section 2) and other mechanical devices including mixers, emulsifiers and ball mills, we concluded that it is impossible to break them up by any conventional means of disintegration.

3.3. Stirred-media milling with micron-sized beads

The unusual resistance of core aggregates against even the strongest sonication available prompted us to seek a mechanical means to destroy the aggregates, and we chose the stirred-media milling for this purpose using micron-sized ceramic beads as the source of attri-

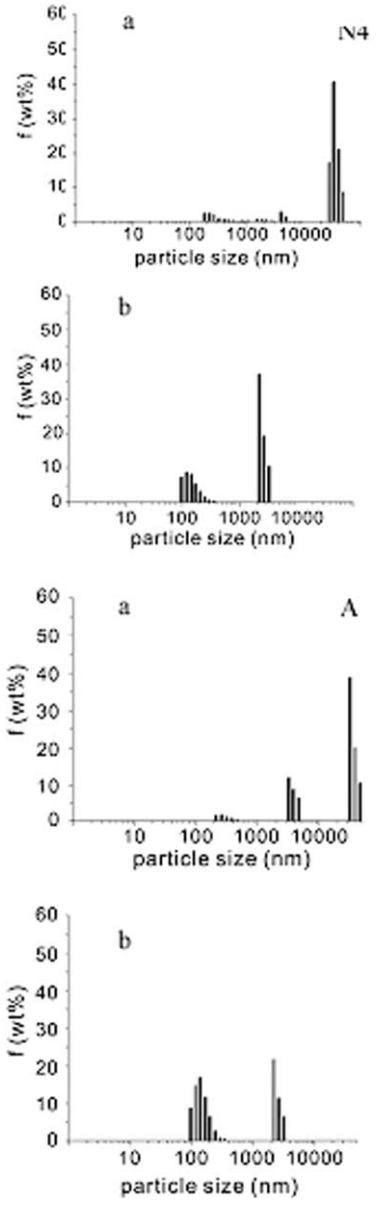

Fig. 2. Particle-size distribution determined by DLS method of nanodiamond samples *N4* and *A* before (upper) and after sonication in 240 W sonication washing bath for 4 h (lower).

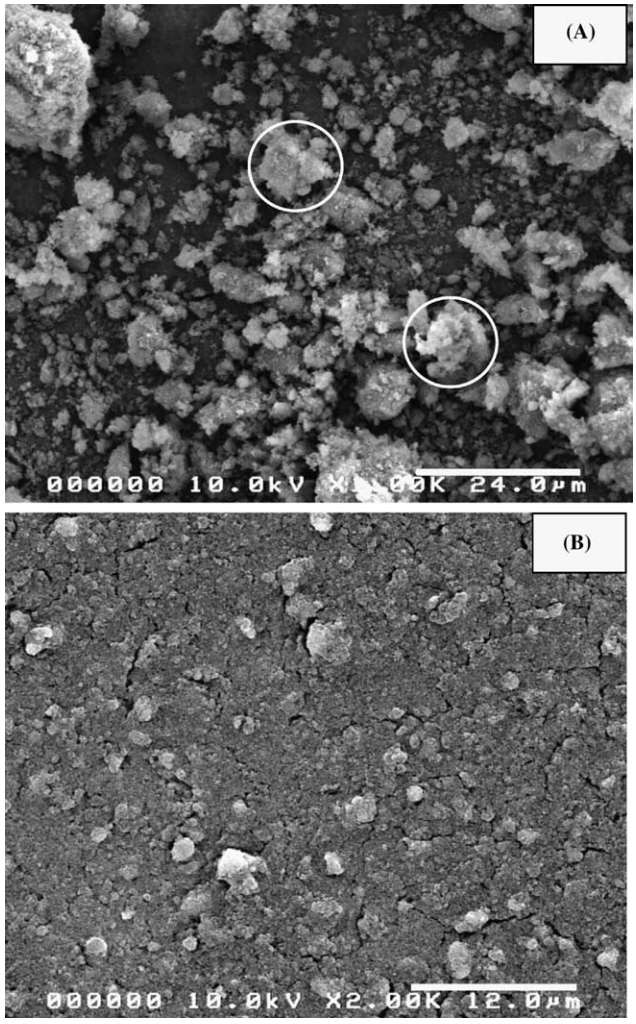

Fig. 3. SEM photographs of nanodiamond sample *N4*. (A) Pristine, the circles show exemplary agglomerates (10.0 kV, ×1000, scale bar = 24 μm), (B) After sonication (240 W, 4 h), the particle size decreased well below 1 μm, but the support is almost completely covered with the diamond powder, hence it is not visible here (10.0 kV, ×2000, scale bar = 12 μm).

tion force [20]. Slurries of pristine samples of *A* and *B* in water were subjected to the stirred-media milling in a self-made mill under high-speed rotation, using a large excess of 0.1 mm silica beads (see Section 2.3). The resulting suspensions exhibited dark colour and turbid appearance but became more viscous than before milling. When the milled slurries were subjected to sonication after diluting to 0.2% with water, the suspension quickly turned transparent! As shown in Fig. 4, DLS particle-size distribution of a milled suspension of *B* initially showed a broad peak centred at around 105 nm, but the average size decreased significantly upon sonication: 10 nm in 5 min, 6.9 nm in 15 min, and eventually 5.3 nm in 1 h. In a separate sonication of more dilute suspension (0.1%) still smaller particle size of 4.5 nm was obtained. Commercial sample *A* reached to 41 nm after milling/sonication but no further reduction of particle size occurred upon continued sonication. Hence only *B* is mentioned below.

To our surprise, the transparent aqueous colloids of primary particles of nanodiamond thus prepared are stable at room temperature when left standing in a closed vessel under stray light, without the addition of any dispersant: turbidity or precipitation was hardly observed for at least a year. In order to see the effect of temperature upon the stability, the colloidal solution was heated at 95 °C by immersing into a boiling bath for 4 h. DLS measurement gave almost a single peak with a maximum distribution at 17 nm (Fig. 5). Hence

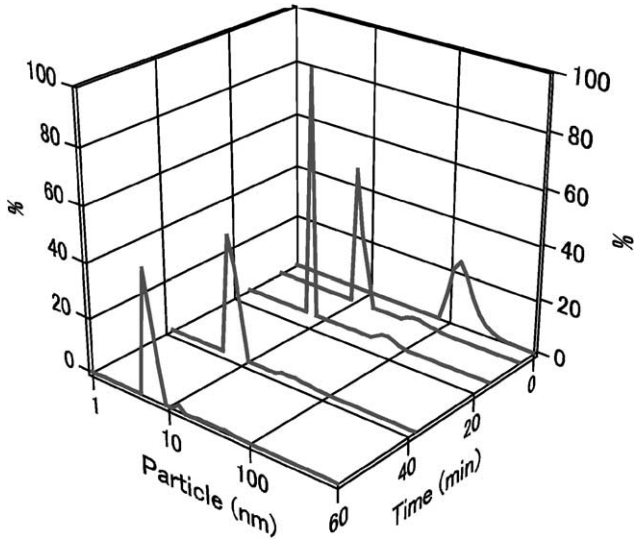

Fig. 4. DLS particle size distribution of nanodiamond sample *B* after stirred-media milling with 0.1 mm SiO_2 beads followed by sonication of the diluted suspension for up to 1 h (0.3 wt.%, 400 W Sonorod, 0.5 s pulse). Ordinate denotes accumulated wt.%.

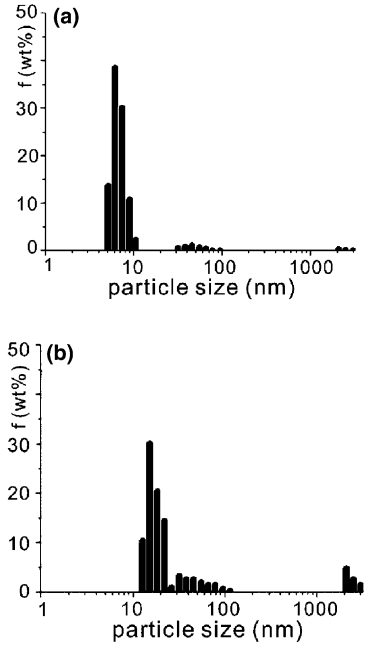

Fig. 5. Stability of DUNCD solutions upon heating: (a) original aq. solution, (b) aq. solution after heating for 4 h at 95 °C.

we conclude that the colloidal solution of primary nanodiamond particles is considerably resistant against heating. In contrast, however, removal of wet medium led to disastrous outcome: upon evaporation of water under vacuum, and re-suspending the resulting powder in water, we obtained only the aggregates of 2.3 μm in diameter.

Nevertheless, we were able to take HRTEM pictures of well-dispersed primary particles by quickly evaporating water from a drop of slurry spread over the carbon-coated copper net of a sample holder in high vacuum (Fig. 6). But still it is difficult to prove the complete de-aggregation of the core aggregates by HRTEM alone as the primary particles re-aggregate rapidly upon solvent removal. Fig. 6c shows the diffraction pattern of a milled sample evidently indicating the diamond character of the particles.

In view of the well-recognized danger of contamination with bead material in the stirred-media milling, we subjected a milled sample of *B* to fluorescence X-ray analysis. The results demonstrated that Si content in *B* increased from 0.05% before milling to 2.5% after milling, which corresponds to 4.9% contamination in terms of SiO_2. FT-IR of the dried residue from the milled suspension displayed a new and intense peak at 1098 cm^{-1}, the Si–O–Si asymmetric stretch absorption. In this regard, SiO_2 may not necessarily be the best material for the present purpose.

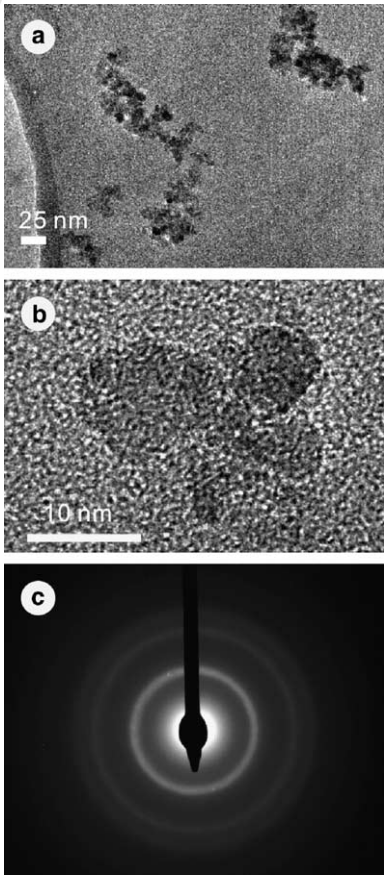

Fig. 6. TEM (200 keV) photograph of beads-milled DUNCD *B*: (a) low magnification, (b) diamond nanoparticles on carbon film and (c) electron diffraction pattern. Note: Due to the fact that immediate reaggregation occurs upon solvent removal it is difficult to image isolated particles. The aggregate in (b) probably formed upon drying.

4. Discussion

4.1. What is special about core aggregates?

Why are core aggregates so hard to disintegrate whereas larger ones are not? Before presenting our interpretation to this question, let us define the three major events that occur during the deposition of carbon atoms from detonation mixture:

(1) *Growth of diamond crystals* (section B in Fig. 7). After the explosion, the *excess* or *unburned* carbon atoms from explosive molecules are engulfed into the rapidly advancing shock wave and exposed to high-temperature/high-pressure conditions corresponding to the diamond region in the carbon phase diagram to begin the diamond growth process. The uniform size-distribution of diamond nanoparticles, as we have seen in TEM pictures and particle-size analysis of primary particles (Figs. 5a and 6), suggest simultaneous formation of a large number of diamond nuclei all at once during a very short period of time.

(2) *Diamond-to-graphite conversion on the surface of diamond particle* (section C in Fig. 7). When T, p parameters in the diamond growth space reach the region of stable graphite, all of the diamond crystals suddenly stop to grow. We mention here two events that are believed to occur after this point. One is the formation of graphitic structures over the surfaces of nanodiamond particles. Two types of structures have been observed. One is the graphitic ribbons with turbostratic structure [24], suggested to arise from carbon redistribution process [25]. Under our own eyes (Fig. 1a), we see highly defective and curved graphitic layers. The other form is more or less spherical graphitic shell as the result of diamond-to-graphite phase transition (bucky diamond [26]), and this phenomenon has been confirmed by separate heating experiments of NDA [27]. However, it must be noted that all these previous experiments were carried out, not on the primary particles, but on the agglomerates. The other event is the formation of spiral subnano-particles containing up to several hundred sp^2-carbon atoms, or *soot embryos* [28].

(3) *Formation of soot-like aggregates* (section D in Fig. 7). As T and p keep decreasing the soot embryos grow into spherical but defective carbon nanoparticles. When the particle diameters reach 10–20 nm, they begin to combine each other into larger clusters, or '*aggregate structure*' as these are called in the area of soot technology [29]. It is likely that the structure includes here bucky diamond particles to form a composite assembly as illustrated in Fig. 8 containing diamond particles with a more or less pronounced graphitic shell, soot structures and also graphitic ribbon-like structures.

We propose that, when a core aggregate is freshly formed, it should have composite structures as illustrated in Fig. 8. This proposal is well supported by the HRTEM image of *N2* (Fig. 1a), wherein both graphitic ribbon-like structure and diamond core are well visible. It should be emphasized that we see only the suface of sample by TEM but not the inside of aggregates. The non-diamond carbons including the invisible amorphous carbons on the surface are largely removed during the nitric acid oxidation step, but the acid-washed products are still aggregated as partly seen in Fig. 1b and c, and also shown in the particle-size distribution (Fig. 2b). A likely interpretation for the failure of complete disintegration during the oxidation reaction will be to invoke a diffusion-limiting slow surface reaction. We are at the moment compelled to assume that the inherently slow oxidation reaction proceeds through the surface only but never work to disintegrate the aggregates

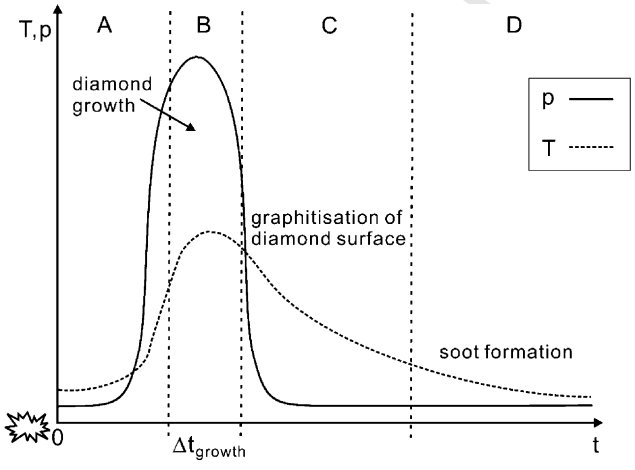

Fig. 7. Events taking place after oxygen-deficient detonation (at $t = 0$) at a position x in the sample. Initial rapid drop in pressure will be followed by slow decrease in temperature resulting in diamond cores with graphitic ribbons and surrounding soot.

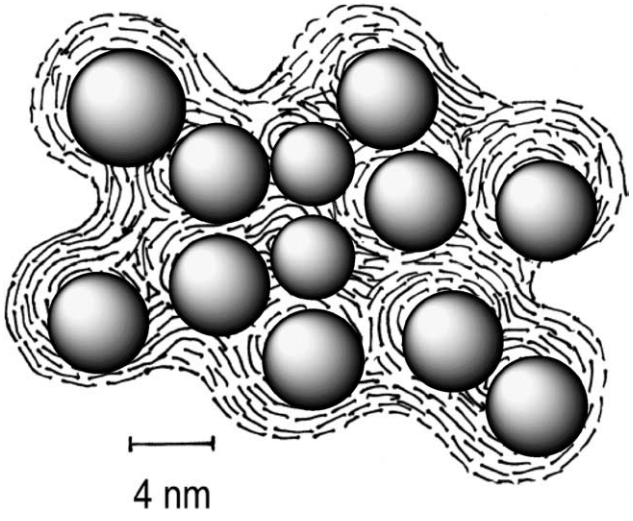

Fig. 8. A simplified model of core aggregate in NDA. Primary particles of cubic diamond crystals are represented by spheres, embedded in the 'aggregate-structure' of soot.

by breaking up the bridging interparticle C–C bonds in the inside of aggregates. The assumption rationalizes the use of brute-force method of the stirred-media milling in order to break up these bonds inside the aggregates. In view of the unprecedented tight bonding of core aggregates, we should reserve the terminology of 'aggregation' to the *van der Waals* type of physical assemblies and use the new terminology like 'agglutination' to the core aggregates that we encountered here.

4.2. Disintegration mechanism

It is interesting to note that the size-range of the grape-like aggregates in commercial carbon black of the super anti-abrasion type or of ASTM N110, prepared at the highest temperature (1800–2000 °C) for the shortest combustion time, falls within the range of 100–200 nm and agrees with the size of our core aggregates [28]. However, it is not yet clear how the beads of 0.1 mm in diameter destroyed such small core aggregates of 100 nm in size: the beads are 1000 times larger than the aggregates. The milling mechanism may not necessarily involve head-on crushes, but mainly works through shearing action in the fast turbulent flow [20].

One notable aspect in the destruction of the core aggregates is that the stirred-media milling did not immediately reach the primary particles (Fig. 4). It seems that the direct effect of milling was to loosen the core structure (Fig. 8), for example by producing cracks at the weak portions of the core aggregate, especially the interparticle bridges. It is likely that the large size of beads compared to the interparticle structure prevented further approach of beads, and the final push by means of cavitation generated by modest sonication was needed to isolate the primary particles. On the other hand, it is unreasonable to assume that the once formed primary particles during milling assemble again to the 105 nm aggregates, which were then disintegrated readily into primary particles.

4.3. Other points of interest

One other novel observation we made in this work is the discrete distribution of particle-size in NDA and DUNCD, which is confined to four constant size-domains, 4–5, 100–200, 2000, and 20,000 nm (Table 3). A number of factors involving relative stabilities, shape, mechanism and rate of formation and disintegration, and interaction with dispersion medium (solvation) exert influence upon the consecutive transformation of aggregates and agglutinates. The most interesting for nano-science would be the back aggregation of pure DUNCD particles, as this is the key to control the dispersion of nanoparticles in general. Once the purification is completed, experimental analysis as well as simulation of aggregation in DUNCD particles will become possible.

Table 3
Classification of particle assemblies in detonation nanodiamond

Equilibria	Average diameter, nm	Volume ratio[a]			Mode of assembly
Primary particle	4.4	(1)			Nano-agglutination
Core aggregate	100	8000	(1)		Nano-aggregation
Intermediate aggregate	2000	9×10^7	10,000	(1)	Micron-agglutination
Agglomerate	20,000	9×10^{10}	10^7	1000	Micron-aggregation

[a] Approximate relative sizes of aggregates compared under three different standards, primary particle (3rd column), core aggregate (4th column), and intermediate aggregate (5th column). Also corresponds to approximate ratios of particle numbers. For example, the 3rd column gives the numbers of primary particles in a core aggregate (ca 8000), etc.

We are aware of the fact that other popular nanocarbon particles obtained by bottom-up synthesis are all tight assemblies formed by the agglutination mechanism. Notable examples include carbon blacks, carbon nanohorns. It is expected that stirred-media milling should be useful to disintegrate these aggregates into isolated primary nanoparticles as well.

Acknowledgement

Work described here is partially supported by JSPS, NEDO and Futaba Corporation. A.K. gratefully acknowledges postdoctoral fellowships from the Humboldt Foundation and the JSPS, 2000–2002, and a Liebig scholarship of the Fonds der Chemischen Industrie. We are indebted to the Netsuren Co. for carrying out stirred milling experiments for us, Dr. H. Oka for some of the TEM pictures of the primary particles and to T. Ogawa, F. Villers and M. Takahashi for technical assistance. We gratefully acknowledge the referee's illuminative comments on the history of nanodiamond discovery and the recommendation of ref. [1].

References

[1] Danilenko VV. The history of the nanodiamond discovery. Book of Abstract, First Int Symp, Detonation Nanodiamonds, July 7–9, 2003, St Petersburg, Russia, p. 27Danilenko VV. Synthesis and sintering of diamond by explosion. Moscow, Energoatomizdat, 2003, p. 138.
[2] Shenderova OA, Zhirnov VV, Brenner DW. Carbon nanostructure. Crit Rev Solid State Mater Sci 2002;27:227–356.
[3] Aleksenskii AE, Baidakova MV, Vul' AY, Siklitskii VI. The structure of diamond nanoclusters. Phys Solid Stat 1999;41:668–71.

[4] Gruen D. Ultrananocrystalline diamond films from fullerene precursors. In: Ōawa E, editor. Perspectives of Fullerene Nanotechnology. Dortrecht: Kluwer Academic Publ.; 2002.
[5] Lyamkin AI, Petrov EA, Ershov AP, Sacovich GV, Staver AM, Titov VM. Production of diamond from explosives (in Russian). Sov Phys Dokl 1988;33:705–6;
See also Greiner RN, Phillips DS, Johnson JD, Volk F. Diamonds in detonation soot. Nature 1988;333:440–2.
[6] Vul' A, Dolmatov V, Shenderova O. Bibliography index of detonation nanodiamonds and related materials. St. Petersburg: Ioffe Physico-Technical Inst.; 2003.
[7] Harlow G, editor. The Nature of Diamonds. Cambridge: Cambridge Univ. Press; 1998.
[8] Hazen RM. The Diamond Makers. Cambridge: Cambridge Univ. Press; 1999.
[9] Wilks WJ, Wilks E. The properties and applications of diamond. Stoneham, MS: Butterworth-Heinemann; 1995.
[10] Sakovich GV, Gubarevich VD, Badaev FZ, Brylyakov PM, Besedina OA. Aggregation of diamonds obtained from explosives. Dokl Akad Nauk SSSR 1990;310:402–4.
[11] Chiganova GA. The effect of particle hydration on the aggregation stability of ultradispersed diamond hydrosols. Colloid J 1997;59:87–9.
[12] Chiganova GA. Aggregation of particles in ultradispersed diamond hydrosols. Colloid J 2000;62:238–43.
[13] Lin EE. Aggregation of crystalline clusters in the shock wave front propagating through condensed species. Sov J Chem Phys 1994;12:404–9.
[14] Aleksenskii AE, Osipov VY, Dideykin AT, Vul' AY, Adreaenssens GJ, Afanasev VV. Ultradisperse diamond cluster aggregation studied by atomic force microscopy. Tech Phys Lett 2000;26:819–21.
[15] Rao CNR, Müller A, Cheetham AK, editors. The chemistry of nanomaterials, vol. 1—2. Weinheim: WILEY-VCH; 2004.
[16] Poole Jr CP, Owens FJ. Introduction to nanotechnology. New Jersey: Wiley-Interscience; 2003.
[17] Rotello V, editor. Nanoparticles—building block for nanotechnology. New York: Kluwer Academic/Plenum Press; 2004.
[18] Dahl JE, Liu SG, Carlson RMK. Isolation and structure of higher diamondoids, nanometer-sized diamond molecules. Science 2003;299:96–9.
[19] Vereshchagin AL. Japanese Patent 2,799,337. Materials containing artificial diamond and their production method. July 10, 1998; See also Donnet JB, Lemoigne C, Wang TK, Peng CM, Samirant M, Eckhardt A. Synthesis of nanodiamond via explosives and shock waves. Bull Soc Chim Fr 1997;134:875–90.
[20] Morrison ID, Ross S. Colloidal dispersions. New York: Wiley; 2002. Chapter 5.5.
[21] Cullity BD, Stock SR. Elements of X-ray diffraction. Upper Saddle River, NJ: Prentice Hall; 2001. Chapter 12.
[22] Berne BJ, Pecora R. Dynamic light scattering with applications to chemistry, biology and physics. Mineola, NY: Dover; 2000.
[23] Alargova RG, Deguchi S, Tsuji K. Stable colloidal dispersions of fullerenes in polar organic solvents. J Am Chem Soc 2001;123:10460–7.
[24] Kuznetsov VL, Chivilin AL, Moroz EM, Kolomiichuk VN, Shikhutdinov ShK, Butenko YuV, et al.. Effect of explosion conditions on the structure of detonation soots: ultradisperse diamond and onion carbon. Carbon 1994;32:873–82.
[25] Kuznetsov VL, Butenko YuV, Zaikovskii VI, Chuvilin AL. Carbon redistribution process in nanocarbons. Carbon 2004;42:1057–61.
[26] Raty JY, Galli G, Bostedt C, van Buuren TW, Terminello LJ. Quantum confinement and fullerenic-like surface reconstructions in nanodiamond. Phys Rev Lett 2003;90:037401.
[27] Baidakova MV, Siklitsky VI, Vul' AY. Ultradisperse diamond nanoclusters. Fractal, structure and diamond-graphite phase transition. Chaos, Solitons & Fractals 1999;10:2153–63.
[28] Ozawa M, Goto H, Kusunoki M, Ōsawa E. Continuously growing spiral carbon nanoparticles as the intermediates in the formation of fullerenes and nano-onions. J Phys Chem B 2002;106:7135–8.
[29] Donnet JB, Bansal RC, Wang MJ. Carbon black, science and technology. second edition.. NY: Marcel Dekker; 1993.